

Supporting Information

Ohmic contact interface in the self-surface reconstructed Ni₄Mo/MoO₂ heterostructure for achieving effective alkaline electrocatalytic water splitting

Amarnath T. Sivagurunathan^{a,1}, T. Kavinkumar^{b,1}, and Do-Heyoung Kim^{a}*

^aSchool of Chemical Engineering, Chonnam National University, 77 Yongbong-ro, Gwangju 61186, Republic of Korea.

^bCentre for Energy and Environment, Department of Physics, Karpagam Academy of Higher Education, Coimbatore 641021, India.

*Corresponding author's email: kdhh@chonnam.ac.kr

Tel. (office): +82-62-530-1894

1 – Equal Contribution

Characterizations

X-ray diffraction (XRD) analysis was analyzed using a Rigaku X-ray diffractometer with CuK α radiation. The morphology and microstructure of the samples were examined using high-resolution scanning electron microscopy (HR-SEM; JEOL JSM-7500F) and transmission electron microscopy (TEM; TECNAI G2 F20 TEM system). X-ray photoelectron spectroscopy (XPS) was done using an ESCALAB-MKII system (VG Scientific Co.). XPS had an Al K alpha source, and the results had been characterized by the Fityk software. Gaussian as a fitting function was used to characterize the XPS results. Inductively coupled plasma optical emission spectroscopy (ICP-OES, iCAP7400DUO, Thermo Scientific) analysis was performed by dissolving the electrodes (1 cm²) in 10 ml of nitric acid for 72 h. The resulting solution was diluted before analysis. Laser Raman spectrophotometer (*NRS-5100*) analysis was carried out at atmospheric condition with a laser excitation wavelength of 532.13 nm with an exposure of 5 s.

Water-splitting measurements

The electrocatalytic performance of the as-prepared samples on NF was determined using a three-electrode cell in which a Mercury/mercury oxide electrode (Hg/HgO) and Pt foil were employed as the reference and counter electrodes, respectively, for the OER, while an Hg/HgO and graphite rod were used as the reference and counter electrodes, respectively, for the HER. Data were acquired using an electrochemical workstation (WonATech WBCS30000). Linear sweep voltammetry (LSV) measurements were conducted at 2 mV s⁻¹ for the OER and HER in 1 M KOH. Electrochemical impedance spectroscopy (EIS) measurements were taken using a Parstat 3000 workstation (0.01 Hz to 100 kHz with a 10-mV amplitude). Gas chromatography (074-594-P1E Micro GC Fusion, INFICON) was used to determine the amount of gaseous products. All of the

potentials were calibrated to the reversible hydrogen electrode (RHE) using Eq. (9), while η was obtained using Eq. (10), and the Tafel slope was calculated using Eq. (11):

$$E_{\text{RHE}} = E_{\text{Hg/HgO}} + 0.059 \text{pH} + 0.098 \quad \dots \quad (9)$$

$$\eta = E_{RHE} - 1.23 \text{-----(10)}$$

Calculation of number of surface-active sites (N_A)

Associated charge with the reduction peak (Q) can be calculated using the following expression:

$$Q = \frac{\int I \, dV}{v}$$

where Q (C) is the total charge associated with the reduction peak and v (V/s) is the scan rate. For simplicity, we assume that all the surface redox reactions are single electron transfer reactions.

Then, the number of electrons calculated above is the number of surface-active sites (N). $q = 1.602 \times 10^{-19}$ C.

$$N = \frac{Q}{q}$$

Electrochemical active surface area (ECSA) calculation

The electrochemical active surface area, which can be determined from the following formula:

$$\text{ECSA} = (\text{specific capacitance} / 40 \mu\text{F cm}^{-2}) \text{ cm}^2$$

Where C_{dl} represents the specific capacitance, and $40 \mu\text{F cm}^{-2}$ is a constant to convert capacitance to ECSA. The specific capacitance can be converted into an electrochemical active surface area (ECSA) using the specific capacitance value for a flat standard with 1.0 cm^2 of real surface area.

Turnover frequency calculation

TOF is the number of times of reaction per unit time and unit active site. Since the exact specific ratio of our hybrid catalyst is unknown, the molar weight cannot be calculated exactly. So, we calculated the number of electrons consumed in the electrode reaction in order to find the number of surface-active sites. To calculate the per-site turnover frequency (TOF), we used the following formula according to previous reports.

$$TOF \text{ per site} = \frac{\text{Total Hydrogen Turn Overs}/\text{cm}^2 \text{ geometric area}}{\text{No. of Surface active sites } / \text{cm}^2 \text{ geometric area}}$$

The number of total hydrogen turn overs is calculated from the current density using the following equation:

$$\begin{aligned}\#_{H_2} &= \left(j \frac{mA}{cm^2} \right) \left(\frac{1C s^{-1}}{1000 mA} \right) \left(\frac{1 mol e^-}{96485.3 C} \right) \left(\frac{1 mol H_2}{2 mol e^-} \right) \left(\frac{6.022 \times 10^{23} H_2 \text{ molecules}}{1 mol H_2} \right) \\ &\quad \frac{H_2/s}{cm^2} \text{ per } \frac{mA}{cm^2}\end{aligned}$$

The number of total oxygen turn overs is calculated from the current density using the following equation:

$$\begin{aligned}\#_{O_2} &= \left(j \frac{mA}{cm^2} \right) \left(\frac{1C s^{-1}}{1000 mA} \right) \left(\frac{1 mol e^-}{96485.3 C} \right) \left(\frac{1 mol O_2}{4 mol e^-} \right) \left(\frac{6.022 \times 10^{23} O_2 \text{ molecules}}{1 mol O_2} \right) \\ &\quad \frac{H_2/s}{cm^2} \text{ per } \frac{mA}{cm^2}\end{aligned}$$

Table S1. Fitted data of electrochemical impedance spectra data shown for as prepared electrode

Electrocatalyst	HER (at -1.1 V vs. Hg/HgO)		OER (at 0.25 V vs. Hg/HgO)	
	R _S (ohm)	R _{CT} (ohm)	R _S (ohm)	R _{CT} (ohm)
NiMoO ₄	1.555	8.166	1.471	1.151
Ni ₄ Mo-MoO ₂	1.423	5.003	1.317	0.808

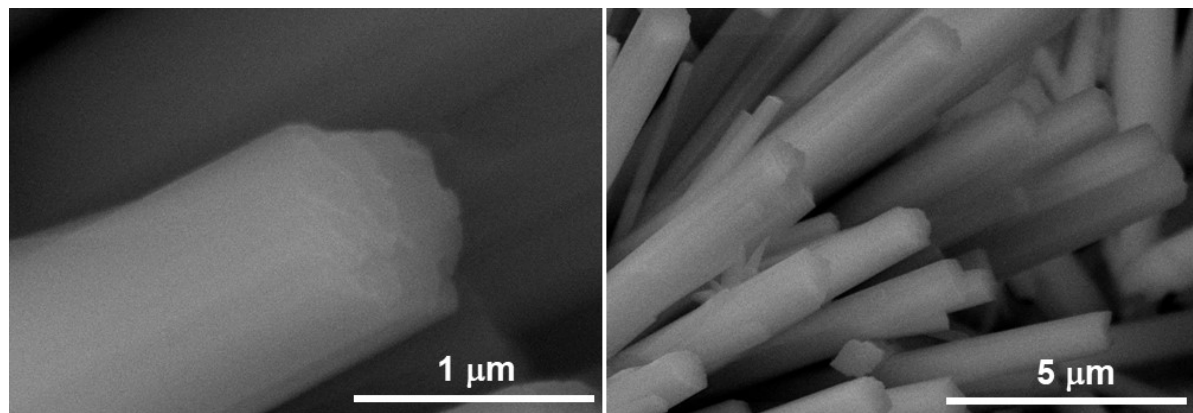


Fig. S1 HR-SEM images of NiMoO₄ electrode.

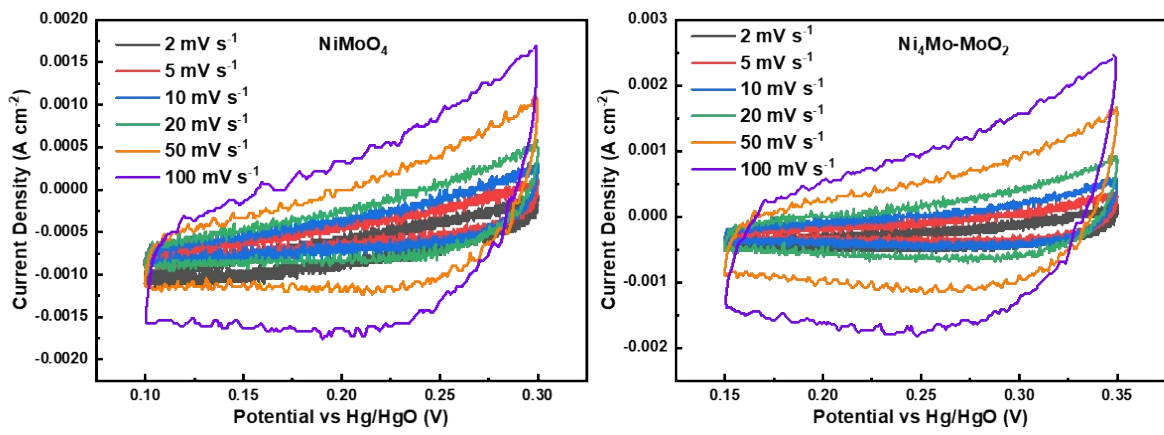


Fig. S2 CV profile of non-faradaic regions of (a) NiMoO_4 , (b) $\text{Ni}_4\text{Mo-MoO}_2$ electrodes respectively

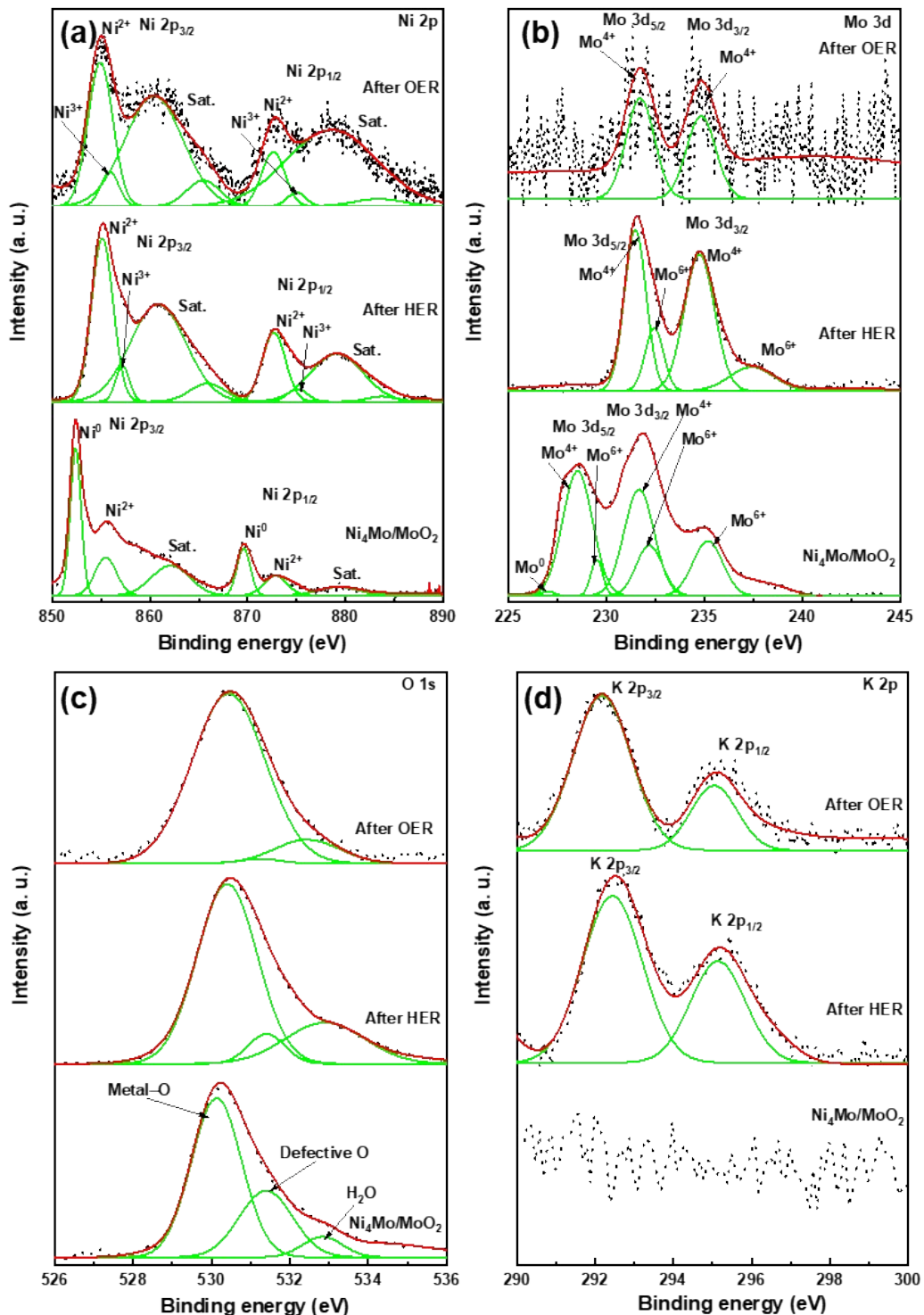


Fig. S3 XPS spectra after OER and HER of $\text{Ni}_4\text{Mo}/\text{MoO}_2$ electrode: (a) Ni 2p, (b) Mo 3d, (c) O 1s, and (d) K 2p.

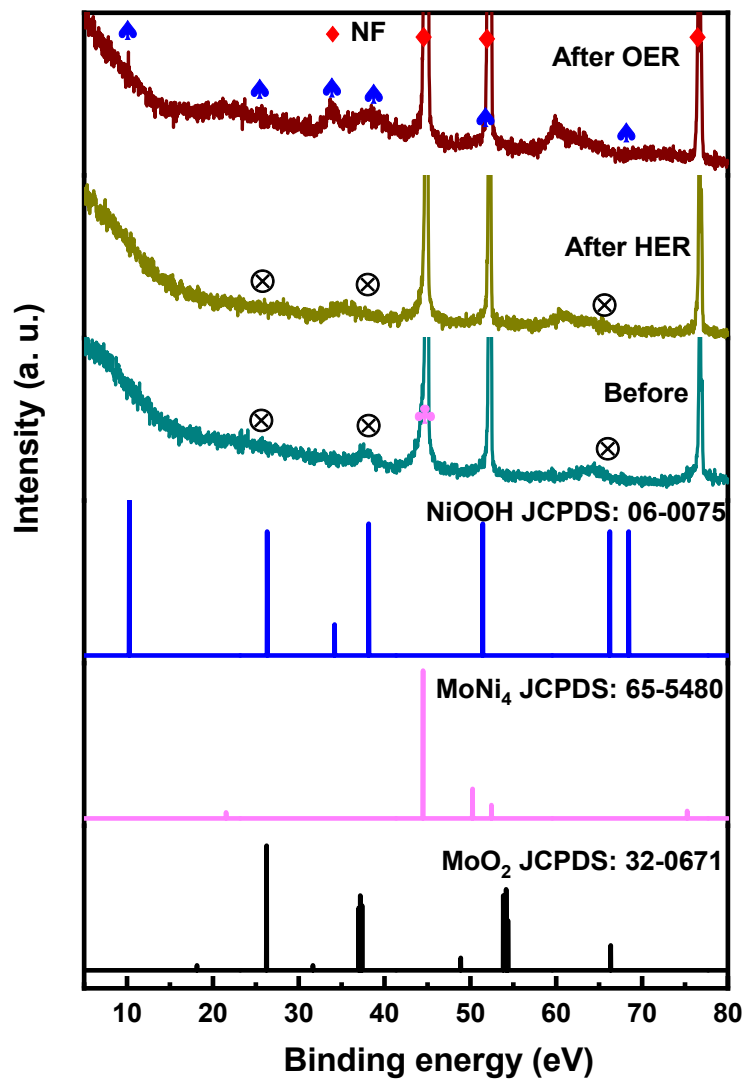


Fig. S4 XRD patterns of $\text{Ni}_4\text{Mo}/\text{MoO}_2$ catalyst before and after HER/OER process.

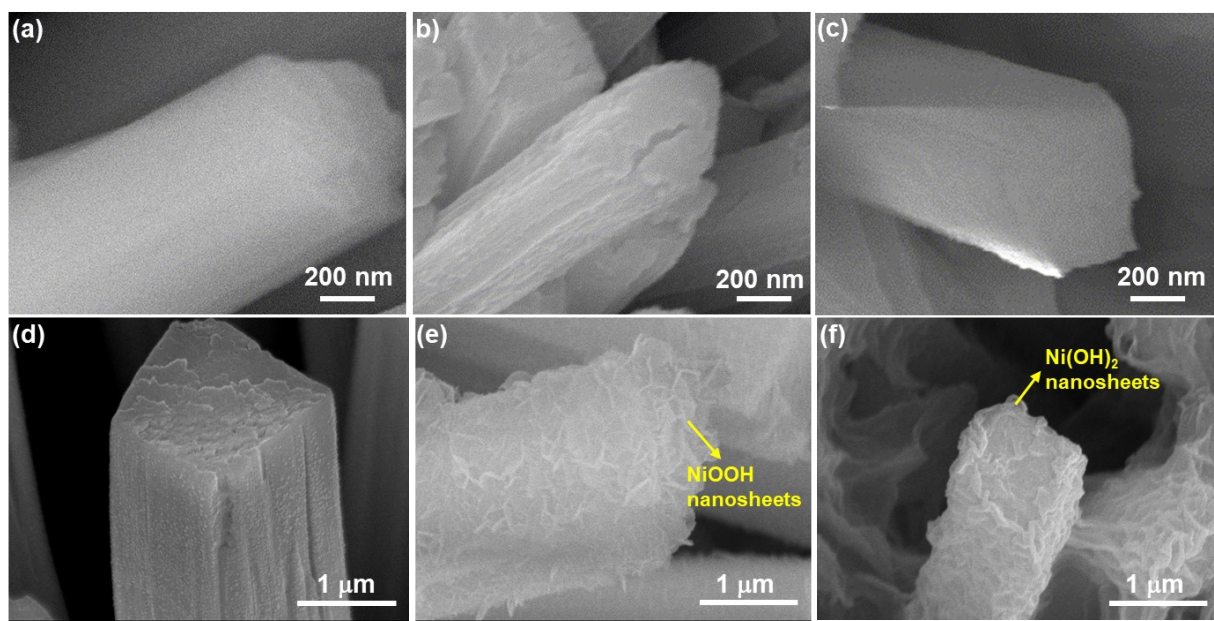


Fig. S5 HR-SEM images of (a) NiMoO_4 , (b) NiMoO_4 -After OER stability, (c) NiMoO_4 -After HER stability, (d) $\text{Ni}_4\text{Mo}/\text{MoO}_2$, (e) $\text{Ni}_4\text{Mo}/\text{MoO}_2$ -After OER stability, and (f) $\text{Ni}_4\text{Mo}/\text{MoO}_2$ -After HER stability.

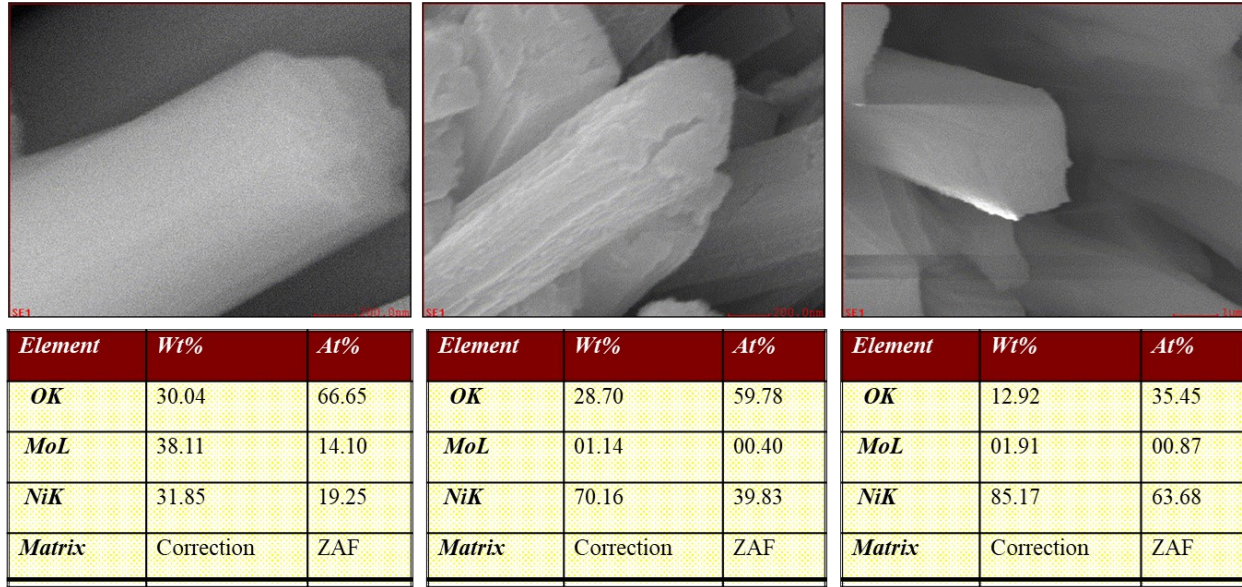


Fig. S6 EDAX analysis on elemental composition of (a) NiMoO₄, (b) NiMoO₄-After OER stability, (c) NiMoO₄-After HER stability.

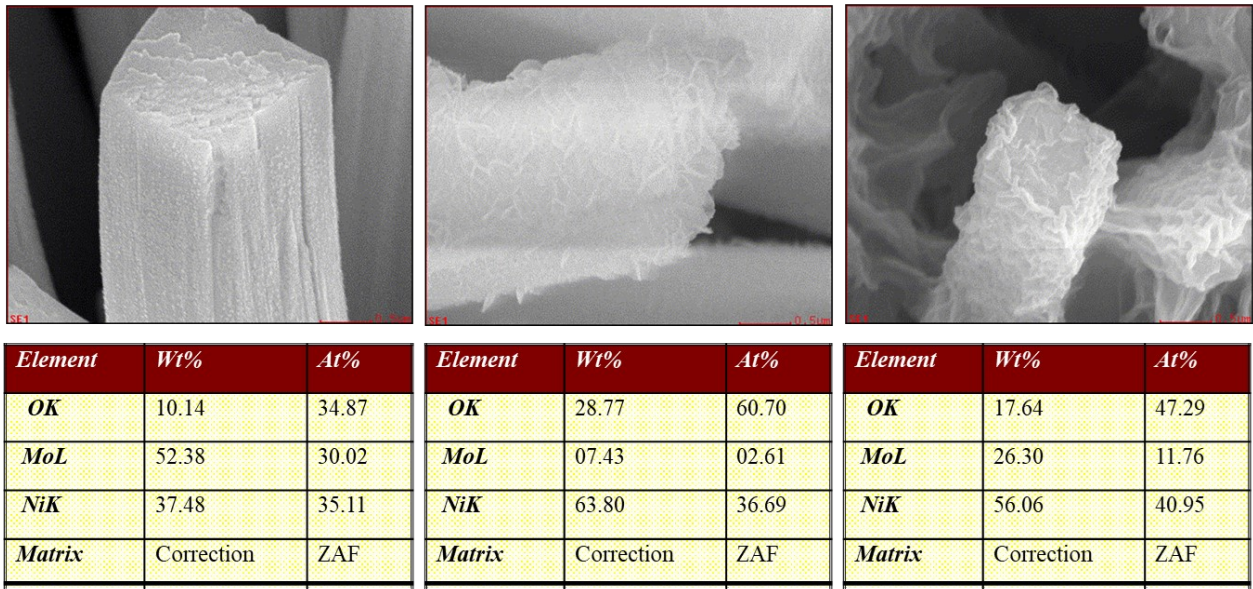


Fig. S7 EDAX analysis on elemental composition of (a) $\text{Ni}_4\text{Mo}/\text{MoO}_2$, (b) $\text{Ni}_4\text{Mo}/\text{MoO}_2$ -After OER stability, and (c) $\text{Ni}_4\text{Mo}/\text{MoO}_2$ -After HER stability.

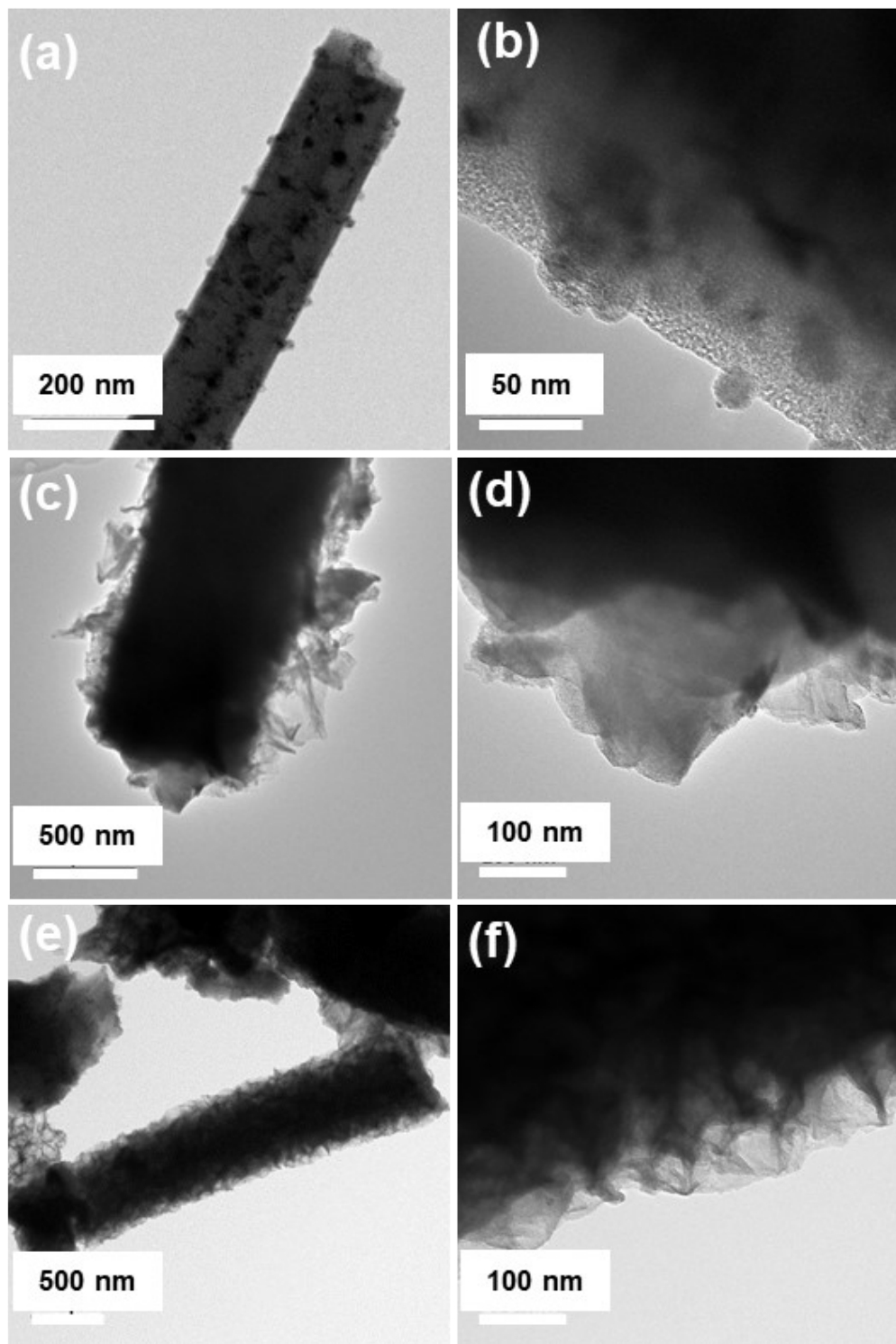


Fig. S8 TEM images of $\text{Ni}_4\text{Mo}/\text{MoO}_2$ catalyst (a, b) before, (c, d) after HER and (e, f) after OER process at different magnifications.

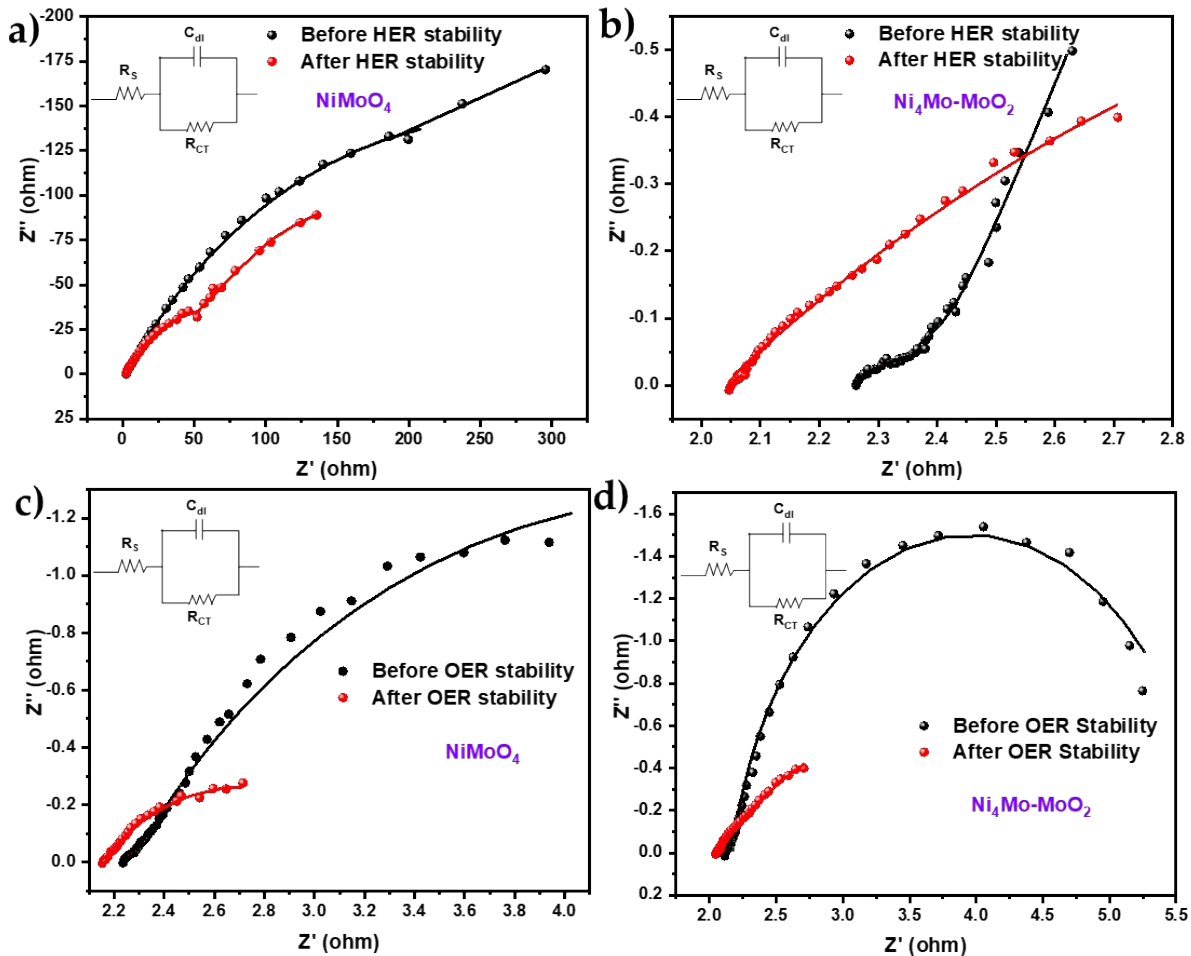


Fig. S9 (a, b) Nyquist plots for the before and after stability HER electrodes NiMoO₄ and Ni₄Mo/MoO₂, respectively at 0 V_{RHE}, with the inset showing the electrochemical equivalent circuit and (c, d) Nyquist plots for the before and after stability OER electrodes NiMoO₄ and Ni₄Mo/MoO₂, respectively at 1.4 V_{RHE}, with the inset showing the electrochemical equivalent circuit.

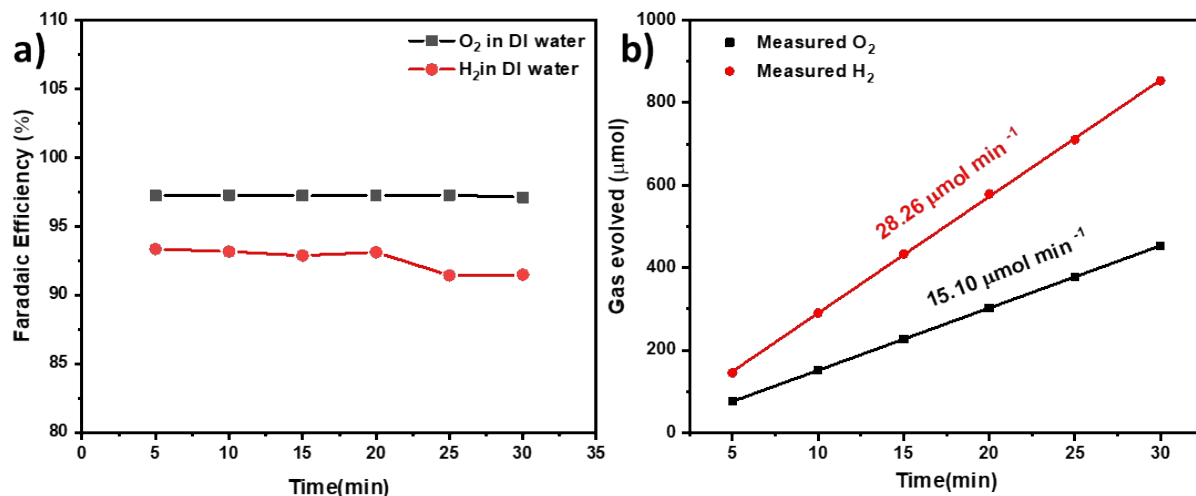


Fig. S10 (a) Gas chromatography results and (b) Faradaic efficiency of the Ni₄Mo/MoO₂ electrode.

Table S2. Fitted data of electrochemical impedance spectra data shown before stability

Electrocatalyst	HER (at 0 V vs. RHE)		OER (at 1.4 V vs. RHE)	
	R _S (ohm)	R _{CT} (ohm)	R _S (ohm)	R _{CT} (ohm)
NiMoO ₄	2.303	534	2.233	4.573
Ni ₄ Mo-MoO ₂	2.241	0.5	2.119	3.57

Table S3. Fitted data of electrochemical impedance spectra data shown after stability

Electrocatalyst	HER (at 0 V vs. RHE)		OER (at 1.4 V vs. RHE)	
	R _S (ohm)	R _{CT} (ohm)	R _S (ohm)	R _{CT} (ohm)
NiMoO ₄	2.25	134	2.156	1.139
Ni ₄ Mo-MoO ₂	2.042	0.389	2.055	1.91

Table S4. Comparison of the electrocatalytic activity for HER in 1 M KOH solution

Catalyst	Electrolyte	Overpotential at 10 mA cm ⁻² (mV)	Tafel slope (mV dec ⁻¹)	Ref.
Ni ₄ Mo/MoO ₂ /NF	1 M KOH	44 mV @ 10 mA cm ⁻² 68 mV @ 50 mA cm ⁻² 89 mV @ 100 mA cm ⁻²	49.5	This work
NiMoS	1 M KOH	78	68	¹
Fe-CoNiP	1 M KOH	110	90.6	²
Ni-Mo-P	1 M KOH	69	108.4	³
Ni _x Fe _{1-x} B	1 M KOH	63.5	56.3	⁴
Ni-Fe-P-B	1 M KOH	220	63	⁵
Mo-NiP _x /NiS _y	1 M KOH	85	177	⁶
Annealed Co–Ni–B@NF	1 M KOH	205	-	⁷
Ni ₄ Mo/MoO ₂ /C-10	1 M KOH	77	100	⁸
Ni-Fe-P@NC/NF	1 M KOH	66	81	⁹
CoP@NF	1 M KOH	195	175	¹⁰
Ni _x B/f-MWCNT	1 M KOH	116	70.4	¹¹
N-MoP	1 M KOH	70	55	¹²
C-Ni ₄ Mo/NiMoO ₄	1 M KOH	76	78	¹³
Ni–P	1 M KOH	52	37.4	¹⁴
RuP ₂ @NPC	1 M KOH	52	38	¹⁵

Table S5. Comparison of the electrocatalytic activity for OER in 1 M KOH solution

Catalyst	Electrolyte	Overpotential at 10 mA cm ⁻² (mV)	Tafel slope (mV dec ⁻¹)	Ref.
Ni₄Mo/MoO₂/NF	1 M KOH	227 mV @ 10 mA cm⁻² 291 mV @ 50 mA cm⁻² 321 mV @ 100 mA cm⁻²	96	This work
Ni-P	1 M KOH	286	44	¹⁴
NiMoO ₄ @Ni ₄ Mo/MoO ₂	1 M KOH	274	63.4	¹⁶
NiMoOS	1 M KOH	262	37.6	¹⁷
Ni ₂ P	1 M KOH	290	-	¹⁸
Co(OH) ₂ /NiMo	1 M KOH	267	72	¹⁹
FeNi-Mo ₂ C/C	1 M KOH	288	38.8	²⁰
CoTe ₂ /CoP	1 M KOH	260	57	²¹
Ni ₃ S ₂ /MoS ₂ /NF	1 M KOH	260	59	²²
Ni-B _i @NB	1 M KOH	302	52	²³
CoP@NF	1 M KOH	317@50	64	²⁴
NiMoN/NF	1 M KOH	230	116	²⁵
Ni-Fe-Mo NTs	1 M KOH	228	41	²⁶
CeO ₂ -NiCoP _x /NCF	1 M KOH	260	72	²⁷
Ni-Fe-P-B	1 M KOH	269	38	⁵

Table S6. Comparison of the electrocatalytic activity for two electrode potential in 1 M KOH solution

Catalyst	Electrolyte	Voltage (V)	Ref.
Ni₄Mo/MoO₂/Ni₄Mo/MoO₂ (iR-uncompensated)	1 M KOH	1.51 V @ 10 mA cm⁻² 1.71 V @ 50 mA cm⁻² 1.91 V @ 100 mA cm⁻² 2.47 V @ 500 mA cm⁻²	This work
NiMoPOx	1 M KOH	1.55 V @ 10 mA cm ⁻²	²⁸
N-NiMoO ₄ /NiS ₂	1 M KOH	1.60 V @ 10 mA cm ⁻²	²⁹
MoP@Ni ₃ P/NF	1 M KOH	1.67 V @ 10 mA cm ⁻²	³⁰
NiFeOx@NiCu	1 M KOH	1.52 V @ 10 mA cm ⁻²	³¹
Mo-doped Ni ₂ P	1 M KOH	1.54 V @ 10 mA cm ⁻²	³²
Co/Mo ₂ C@C	1 M KOH	1.59 V @ 10 mA cm ⁻²	³³
Annealed Co–Ni–B@NF	1 M KOH	1.72 V @ 10 mA cm ⁻²	⁷
Ni–Fe–P–B over CFP	1 M KOH	1.62 V @ 10 mA cm ⁻²	⁵
Ni–P	1 M KOH	1.6 V @ 10 mA cm ⁻²	¹⁴
Ni–Fe–Mo NTs	1 M KOH	1.513 V @ 10 mA cm ⁻²	²⁶
Co ₄ S ₃ /Mo-2 C-N SC	1 M KOH	1.62 V @ 10 mA cm ⁻²	³⁴
P – CoMo ₂ S ₄ /Co ₄ S ₃ –Co ₂ P	1 M KOH	1.55 V @ 10 mA cm ⁻²	³⁵
Ni _x B/f-MWCNT	1 M KOH	1.60 V @ 10 mA cm ⁻²	¹¹
Fe–CoNiP	1 M KOH	1.62 V @ 10 mA cm ⁻²	²
RuP/CoNiP ₄ O ₁₂ /CC	1 M KOH	1.56 V @ 10 mA cm ⁻²	³⁶
NC/NiMo/NiMoOx	1 M KOH	1.60 V @ 10 mA cm ⁻²	³⁷

References

1. L. Ji, J. Wang, X. Teng, T. J. Meyer and Z. Chen, *ACS Catal.*, 2020, **10**, 412-419.
2. M. Ramadoss, Y. Chen, X. Chen, Z. Su, M. Karpuraranjith, D. Yang, M. A. Pandit and K. Muralidharan, *J. Phys. Chem. C*, 2021, **125**, 20972-20979.
3. B. Zhang, F. Yang, X. Liu, N. Wu, S. Che and Y. Li, *Appl. Catal. B-Environ.*, 2021, **298**, 120494.
4. W. Hong, S. Sun, Y. Kong, Y. Hu and G. Chen, *J. Mater. Chem. A*, 2020, **8**, 7360-7367.
5. W. Tang, X. Liu, Y. Li, Y. Pu, Y. Lu, Z. Song, Q. Wang, R. Yu and J. Shui, *Nano Res.*, 2020, **13**, 447-454.
6. J. Wang, M. Zhang, G. Yang, W. Song, W. Zhong, X. Wang, M. Wang, T. Sun and Y. Tang, *Adv. Funct. Mater.*, 2021, **31**, 2101532.
7. N. Xu, G. Cao, Z. Chen, Q. Kang, H. Dai and P. Wang, *J. Mater. Chem. A*, 2017, **5**, 12379-12384.
8. G. Wei, C. Wang, X. Zhao, S. Wang and F. Kong, *J. Alloy. Compd.*, 2023, **939**, 168755.
9. Y. Wang, S. Zhao, Y. Zhu, R. Qiu, T. Gengenbach, Y. Liu, L. Zu, H. Mao, H. Wang, J. Tang, D. Zhao and C. Selomulya, *iScience*, 2020, **23**, 100761-100761.
10. D. Liang, L. Zhang, W. He, C. Li, J. Liu, S. Liu, H.-S. Lee and Y. Feng, *Appl. Energy*, 2020, **264**, 114700.
11. Z. Y. Xu, J. C. Ren, Q. Meng, X. H. Zhang, C. C. Du and J. H. Chen, *Acs Sustain Chem Eng*, 2019, **7**, 12447-12456.
12. N. Chen, W. Zhang, J. Zeng, L. He, D. Li and Q. Gao, *Appl. Catal. B-Environ.*, 2020, **268**, 118441.

13. M. Gong, W. Zhou, M.-C. Tsai, J. Zhou, M. Guan, M.-C. Lin, B. Zhang, Y. Hu, D.-Y. Wang, J. Yang, S. J. Pennycook, B.-J. Hwang and H. Dai, *Nat. Commun.*, 2014, **5**, 4695.
14. D. Song, D. Hong, Y. Kwon, H. Kim, J. Shin, H. M. Lee and E. Cho, *J. Mater. Chem. A*, 2020, **8**, 12069-12079.
15. Z. Pu, I. S. Amiinu, Z. Kou, W. Li and S. Mu, *Angew. Chem. -Int. Edi.*, 2017, **56**, 11559-11564.
16. J. Zhang, S. Zhang, X. Zhang, Z. Ma, Z. Wang and B. Zhao, *J. Colloid Interface Sci.*, 2023, **650**, 1490-1499.
17. J. Liu, W. Qiao, Z. Zhu, J. Hu and X. Xu, *Small*, 2022, **18**, 2202434.
18. L.-A. Stern, L. Feng, F. Song and X. Hu, *Energy Environ. Sci.*, 2015, **8**, 2347-2351.
19. Q. Zhang, W. Xiao, W. H. Guo, Y. X. Yang, J. L. Lei, H. Q. Luo and N. B. Li, *Adv. Funct. Mater.*, 2021, **31**, 2102117.
20. M. Wang, Y. Wang, S. S. Mao and S. Shen, *Nano Energy*, 2021, **88**, 106216.
21. L. Yang, X. Cao, X. Wang, Q. Wang and L. Jiao, *Appl. Catal. B-Environ.*, 2023, **329**, 122551.
22. C. Wang, X. Shao, J. Pan, J. Hu and X. Xu, *Appl. Catal. B-Environ.*, 2020, **268**, 118435.
23. W.-J. Jiang, S. Niu, T. Tang, Q.-H. Zhang, X.-Z. Liu, Y. Zhang, Y.-Y. Chen, J.-H. Li, L. Gu, L.-J. Wan and J.-S. Hu, *Angew. Chem. -Int. Edit.*, 2017, **56**, 6572-6577.
24. J. Liu, Y. Gao, X. Tang, K. Zhan, B. Zhao, B. Y. Xia and Y. Yan, *J. Mater. Chem. A*, 2020, **8**, 19254-19261.
25. Y. Wang, Y. Sun, F. Yan, C. Zhu, P. Gao, X. Zhang and Y. Chen, *J. Mater. Chem. A*, 2018, **6**, 8479-8487.

26. C. Zhu, Z. Yin, W. Lai, Y. Sun, L. Liu, X. Zhang, Y. Chen and S.-L. Chou, *Adv. Energy Mater.*, 2018, **8**, 1802327.
27. T. Xiong, X. Yao, Z. Zhu, R. Xiao, Y.-w. Hu, Y. Huang, S. Zhang and M.-S. Balogun, *Small*, 2022, **18**, 2105331.
28. F. Kong, L. Sun, L. Huo and H. Zhao, *J. Power Sources*, 2019, **430**, 218-227.
29. L. An, J. Feng, Y. Zhang, R. Wang, H. Liu, G.-C. Wang, F. Cheng and P. Xi, *Adv. Funct. Mater.*, 2019, **29**, 1805298.
30. P. V. Shinde, N. M. Shinde, J. M. Yun, R. S. Mane and K. H. Kim, *ACS Omega*, 2019, **4**, 11093-11102.
31. Y. Zhou, Z. Wang, Z. Pan, L. Liu, J. Xi, X. Luo and Y. Shen, *Adv. Mater.*, 2019, **31**, 1806769.
32. Q. Wang, H. Zhao, F. Li, W. She, X. Wang, L. Xu and H. Jiao, *J. Mater. Chem. A*, 2019, **7**, 7636-7643.
33. S. Yuan, M. Xia, Z. Liu, K. Wang, L. Xiang, G. Huang, J. Zhang and N. Li, *Chem. Eng. J.*, 2022, **430**, 132697.
34. Y. Liu, X. Luo, C. Zhou, S. Du, D. Zhen, B. Chen, J. Li, Q. Wu, Y. Iru and D. Chen, *Appl. Catal. B-Environ.*, 2020, **260**, 118197.
35. K. Dong, D. T. Tran, X. Li, S. Prabhakaran, D. H. Kim, N. H. Kim and J. H. Lee, *Appl. Catal. B-Environ. Energy*, 2024, **344**, 123649.
36. J. Zhao, Y. Zhang, Y. Xia, B. Zhang, Y. Du, B. Song, H.-L. Wang, S. Li and P. Xu, *Appl. Catal. B-Environ.*, 2023, **328**, 122447.
37. J. Hou, Y. Wu, S. Cao, Y. Sun and L. Sun, *Small*, 2017, **13**, 1702018.

